AGU PUBLICATIONS

JGR

Journal of Geophysical Research: Biogeosciences

RESEARCH ARTICLE
10.1002/2013JG002515

Key Points:
- A statistically viable approach to map forest stand age was presented
- A 1 km national forest age map was produced using observations and height data
- Main potential uncertainties for broad-scale applications were discussed

Supporting Information:
- Readme
- Appendices S1–S3

Correspondence to:
W. Ju,
juweimin@nju.edu.cn

Citation:
Zhang, C., W. Ju, J. M. Chen, D. Li, X. Wang, W. Fan, M. Li, and M. Zan (2014), Mapping forest stand age in China using remotely sensed forest height and observation data, *J. Geophys. Res. Biogeosci.*, *119*, 1163–1179, doi:10.1002/2013JG002515.

Received 20 SEP 2013
Accepted 16 MAY 2014
Accepted article online 22 MAY 2014
Published online 13 JUN 2014

Mapping forest stand age in China using remotely sensed forest height and observation data

Chunhua Zhang[1], Weimin Ju[1], Jing M. Chen[1], Dengqiu Li[1], Xiqun Wang[2], Wenyi Fan[3], Mingshi Li[4], and Mei Zan[1]

[1]International Institute for Earth System Science, Nanjing University, Nanjing, China, [2]Planning and Design Institute of Forest Products Industry, State Forestry Administration of China, Beijing, China, [3]College of Forestry, Northeast Forestry University, Harbin, China, [4]College of Forest Resources and Management, Nanjing Forestry University, Nanjing, China

Abstract Forest stand age plays a crucial role in determining the terrestrial carbon source or sink strength and reflects major disturbance information. Forests in China have changed drastically in recent decades, but quantification of spatially explicit forest age at national level has been lacking to date. This study generated a national map of forest age at 1 km spatial resolution using the remotely sensed forest height and forest type data in 2005, as well as relationships between age and height retrieved from field observations. These relationships include biomass as an intermediate parameter for major forest types in different regions of China. Biomass-height and age-biomass relationships were well fitted using field observations, with respective R^2 values greater than 0.60 and 0.71 ($P < 0.01$), indicating the viability of age-height relationships developed for age estimation in China. The resulting map was evaluated by comparison with national, provincial, and county forest inventories. The validation had high regional ($R^2 = 0.87$, 2–8 years errors in six regions), provincial ($R^2 = 0.53$, errors less than 10 years and consistent age structure in most provinces), and plot (R^2 values of 0.16−0.32, $P < 0.01$) agreement between map values and inventory-based estimates. This confirms the reliability and applicability of the age-height approach demonstrated in this study for quantifying forest age over large regions. The map reveals a large spatial heterogeneity of forest age in China: old in southwestern, northwestern, and northeastern areas, and young in southern and eastern regions.

1. Introduction

Forest ecosystems, major contributors to the terrestrial carbon sink in recent decades, play an irreplaceable role in regulating the global carbon balance by reducing the atmospheric CO_2 buildup [*Houghton et al.*, 2000; *Houghton,* 2007; *Bonan*, 2008; *Piao et al.*, 2009; *Pan et al.*, 2011b]. Carbon strength (sink or source) of forest ecosystems is a reflection of past disturbances and nondisturbance factors (climate change, CO_2 concentration, and nitrogen deposition). A number of early studies considered nondisturbance factors in estimating forest carbon budgets, but the effects of forest stand age were ignored due to the lack of quantitative knowledge about age distribution. Forest age is widely recognized as a primary driver of forest structure and function, and affects many components in the forest carbon cycle, including stand biomass [*Pan et al.*, 2004; *Xu et al.*, 2010], live biomass increment and litter decomposition [*Bradford et al.*, 2008; *Xu et al.*, 2012], net primary productivity (NPP) [*Ryan et al.*, 1997; *Chen et al.*, 2002; *He et al.*, 2012], net ecosystem productivity (NEP) [*Song and Woodcock*, 2003; *Grace*, 2004; *Pan et al.*, 2011a], and biophysical properties [*McMillan and Goulden*, 2008]. Recently increasing studies have highlighted that forest age structure is a critical factor determining the carbon strength at various spatiotemporal scales and can be used as a surrogate for major disturbance information such as clear-cut [*Chen et al.*, 2000, 2003; *Ju et al.*, 2007; *Turner et al.*, 2007; *Wang et al.*, 2007, 2011; *He et al.*, 2011; *Zhang et al.*, 2012]. Thus, it is imperative to develop reliable and spatially explicit forest age data for improving forest carbon budget simulation.

Optical remote sensing offers important data for mapping regional forest age according to vegetation spectral signatures and spatial patterns over time [*Lucas et al.*, 1993, 2002]. However, spectral measurements are typically sensitive to stand age at the early stages of forest growth and quickly saturate following canopy closure [*Sader et al.*, 1989; *Fraser and Li,* 2002; *Amiro and Chen*, 2003; *Zhang et al.*, 2004; *Dai et al.*, 2011]. Time series of remote sensing data could be used to extract forest age using change detection techniques, but good quality of long time series data is not guaranteed over large areas [*Drake et al.*, 2011; *Li et al.*, 2014]. Radar measurements, such as those based on interferometric coherence, were used to monitor variations of

forest age. But the resulting age map is also affected by the saturation effects for mature forests [*Drezet and Quegan*, 2007]. Moreover, radar is less species specific than optical methods because the longer wavelength radiation is less sensitive to biochemical properties (such as soil and plant moisture conditions). Ground-based forest inventories directly quantify stand age at sampling plots or age classes in a province. Determination of stand age is, however, an inexact process because averaged or downscaled age in the sampling area cannot provide spatially detailed characterization of age change [*Wang et al.*, 2007; *Vilén et al.*, 2012]. In addition, the inventory approach is restricted by data availability and could not be applied everywhere. Combination of data reflecting forest age from inventories, historical disturbance data (fire scar polygon and harvesting), and optical satellite data is the most promising method for compiling a regional forest age map [*Chen et al.*, 2003; *Pan et al.*, 2011a]. However, this method requires acquisitions of multitemporal data and makes many assumptions. Biometric observations of NPP, biomass, age, and tree height have been widely available in forest ecosystems, which potentially provide age estimates by establishing the relationship between age and other biophysical variables. This method does not need too many assumptions and data, and therefore, it is easy to implement over large areas. The key to the method is to seek suitable age-related variables and develop analytical models for age estimation.

Because forest stand age has considerable spatial variability in China, it is difficult to obtain the wide range of spatially explicit data required for forest age estimation. National forest inventory data (FID) can provide statistical information on areas of different stand origins (natural and planted) in five age classes: young, middle aged, premature, mature, and overmature for dominant forest species in each province across China. In addition, it is implemented once every 5 years, making it very hard to derive explicit age information over space and time. The first national forest age map was produced with 1 km resolution from FID recorded between 1989 and 1993 in 32 provinces of China [*Wang et al.*, 2007]. This map promoted forest carbon budget simulation in China [*Ju et al.*, 2007; *Wang et al.*, 2011]. However, the FID used by *Wang et al.* [2007] could not well reflect grid-based differences of age within a province. *Dai et al.* [2011] compiled a national forest age map at 8 km spatial resolution based on the relationship between provincial mean stand age retrieved from 1994–1998 forest inventories and growing season AVHRR (Advanced Very High Resolution Radiometer) NDVI (Normalized Difference Vegetation Index). The saturation of NDVI with age would definitely result in an underestimation of high stand ages. Therefore, other indicators are required for better quantification of forest age in China.

Forest biomass has a strong relationship with stand age [*Pan et al.*, 2004; *Cienciala et al.*, 2008; *Xu et al.*, 2010], and thus, stand age could be inferred from biomass [*Zheng et al.*, 2004; *Piao et al.*, 2005]. However, large-scale forest biomass estimation is currently still a challenge. *Fang et al.* [2006] elucidated that forest height was an effective proxy of regional biomass in mid to high-latitude forests, implying that light detecting and ranging (LiDAR) techniques can be used to estimate forest biomass based on the relationship of biomass with forest height over large regions. The latest studies with satellite-borne LiDAR have shown that forest height could be mapped with LiDAR satisfactorily from regional to global scales [*Lefsky et al.*, 2007; *Duncanson et al.*, 2010; *Lefsky*, 2010; *Simard et al.*, 2011]. Such forest height maps provide an ideal opportunity for estimating large-scale forest biomass [*Lefsky et al.*, 2005b; *Fang et al.*, 2006] and forest age. Recently, *Simard et al.* [2011] produced a global wall-to-wall canopy height map for 2005 by combining the Geoscience Laser Altimeter System estimates and global ancillary variables (http://lidarradar.jpl.nasa.gov/), which was well consistent with field measurements from 66 FLUXNET sites distributed globally over a broad range of forest types. Given that China currently lacks a reliable national forest height product, the attempt is made here to apply the map created by *Simard et al.* [2011] to estimate forest age in China. The objectives are to (1) demonstrate a viable approach for combining field observations and remotely sensed forest height in order to estimate forest stand age; (2) evaluate a spatially explicit data set of forest age estimated from remotely sensed forest height; and (3) examine the spatial pattern of forest age in China.

2. Data and Methods

Field measurements at 3543 forest plots across China were collected from the literature to establish biomass-height and age-biomass relationships for major forest types in different regions (Figures 1a–1c). The relevant empirical relationships between stand age and forest height were further developed (equation (1)) by using biomass as the transfer parameter, because no general formula is currently available for describing

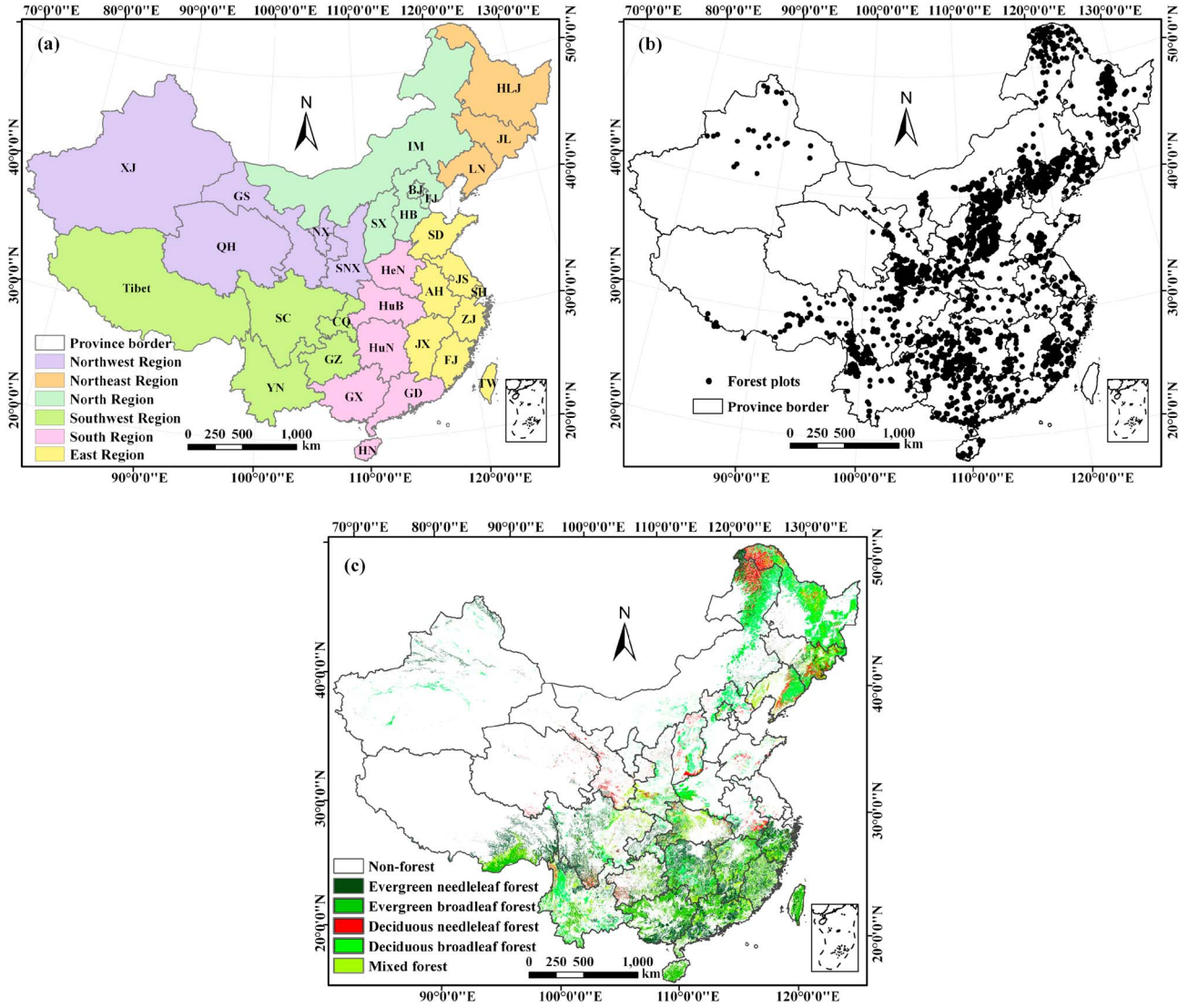

Figure 1. Distributions of forest regions, plots, and forest types in China. (a) Forest regions following *Fang et al.* [2001]; (b) geographical distribution of 3543 forest plots used; (c) spatial distribution of China's forest types in 2005. Northeast region includes Heilongjiang (HLJ), Jilin (JL), Liaoning (LN); North region includes Beijing (BJ), Hebei (HB), Inner Mongolia (IM), Shanxi (SX) and Tianjin (TJ); East region includes Anhui (AH), Fujian (FJ), Jiangsu (JS), Jiangxi (JX), Shandong (SD), Shanghai (SH), Taiwan (TW), and Zhejiang (ZJ); South region includes Guangdong (GD), Guangxi (GX), Henan (HeN), Hainan (HN), Hubei (HuB), and Hunan (HuN); Southwest region Chongqing (CQ), Guizhou (GZ), Sichuan (SC), Tibet, and Yunnan (YN); Northwest region includes Gansu (GS), Ningxia (NX), Qinghai (QH), Shannxi (SNX), and Xinjiang (XJ).

the age-height relationship explicitly. Forest age, defined as a mean age of all trees in a grid cell here, was estimated using an age-height relationship in combination with forest height data.

$$\text{Age} = f_1(\text{Biomass}) = f_1(f_2(\text{Height})) \quad (1)$$

where f_1 is the function describing the relationship between forest age (year) and biomass (Mg ha^{-1}), and f_2 represents forest biomass as a function of forest height (m). The parameters in f_1 and f_2 are fitted using field measurements (Tables 1–3). Finally, forest age is calculated on the basis of height through replacing biomass in function f_1 with function f_2 (Table 4).

2.1. Data

2.1.1. Field Measurement Data

In this study, published data from 3543 sampling plots with a wide range of forest types and plot conditions in China were compiled for fitting parameters in equation (1). The sampling was conducted for the period from 1979 to 2011. Recorded information of sampling plots includes geographic location, forest type,

Table 1. Five Types of Theoretical Stand Growth Model[a]

Model	Formula	Parameter Range	Inflect Point	Function f_1	Source
R	$B=a(1-\exp(-bA))^{1/(1-c)}$	$a, b, c>0$	$A=\ln(1/(1-c))/b$, $B=ac^{1/(1-c)}$	$A=-\ln(1-B^{(1-c)}/a)/b$ $(B<a^{(1/(1-c))})$	*Pienaar and Turnbull* [1973]
M	$B=a(1-b\exp(-cA))$	$a>0, 0<b\le 1, c>0$	–	$A=(\ln(b)-\ln(1-B/a))/c$ $(a(1-b)<B<a)$	*Richer* [1979]
L	$B=a/(1+\exp(b-cA))$	$a, b>0$	$A=b/c$, $B=2/a$	$A=(b-\ln(a/B-1))/c$ $(a/(1+\exp(b))<B<a)$	*Gadow and Hui* [1998]
G	$B=a\exp(-\exp(b-cA))$	$a, c>0$	$A=b/c$, $B=a/e$	$A=(b-\ln(\ln(a/B)))/c$ $(a/\exp(\exp(b))<B<a)$	*Charles* [1932]
K	$B=a\exp(-b/A^c)$	$a, b, c>0$	$A=((c+1)/bc)^{1/c}$, $B=a\exp(-(c+1)/c)$	$A=(b/\ln(a/B))^{1/c}$ $(B<a)$	*Zeide* [1989]

[a]Model identifications are Richards, R; Mitscherlich, M; Logistic, L; Gompertz, G; and Korf, K. f_1 defined in equation (1) represents forest age (A, year) as function of forest biomass (B, Mg ha^{-1}): $A=f_1(B)$, calculation procedures for which were obtained by reversing stand growth models. a, b, and c are fitted parameters of models using field measurements.

standage, stand density, stand volume, mean tree height and diameter at breast height (DBH) for trees with DBH > 4 cm, and biomass of whole trees and their component parts (stems, branches, leaves, and roots) [*Zhang et al.*, 2013].

These plots are evenly distributed in most regions of China except for Xinjiang and the Qinghai-Tibetan Plateau. Forest types and site conditions of the plots in most provinces are diverse (Figure 1b). In Xinjiang and the Qinghai-Tibetan Plateau, however, the sampling plots are sparse. Forests in these regions account for only a small fraction of the national total. Therefore, the lack of enough sampling plots here might have a little impact on the accuracy of the retrieved national forest age map.

2.1.2. Forest Type Map

A 2005 forest type map with a spatial resolution of 1 km in China generated by the Institute of Remote Sensing and Digital Earth, Chinese Academy of Sciences [*Zhang et al.*, 2009], was used to delineate the distribution of forests. In this map, forests were classified into five types (Figure 1c), including deciduous needleleaf forest (DNF), evergreen needleleaf forest (ENF), deciduous broadleaf forest (DBF), evergreen broadleaf forest (EBF), and mixed forest (MF). Overall map accuracy for the classification was 90% [*Zhang et al.*, 2009]. According to the forest type map, the total area of China's forests was about 177.19×10^6 ha in 2005 (excluding Taiwan). This is higher than the value of 155.59×10^6 ha of forest stands reported by the State Forestry Administration [*Chinese Ministry of Forestry*, 2009] because of different definitions of forest stands.

2.1.3. Forest Height Data

The global 1 km canopy height map in 2005 produced by *Simard et al.* [2011] shows a better correspondence with in situ canopy height at 66 FLUXNET sites ($R^2=0.69$ and root-mean-square error (RMSE) = 4.36 m). However, the canopy height estimates are greatly influenced by geographic location and forest heterogeneity. The estimates of *Simard et al.* [2011] are generally higher than those in *Lefsky* [2010] and the ICESat (Ice, Cloud, and land Elevation Satellite) map. In this study, the forest canopy height of *Simard et al.* [2011] was calibrated using measured mean tree height at 263 plots selected from all sampling plots with measurements conducted during 2001–2010 (Figure 2). Due to the limited data availability, forest canopy height values in the northeastern and northwestern regions were calibrated using the same correction coefficient and other regions of China adopted another one. Forest canopy height values match field

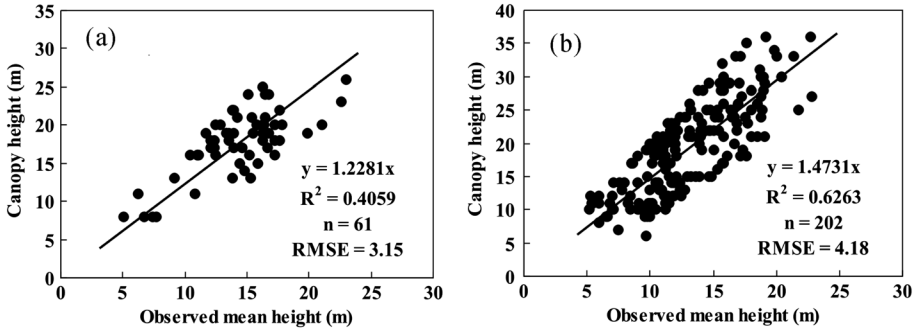

Figure 2. Comparison of forest canopy height values and field measurements in China for (a) the northeast and northwest regions and (b) the east, north, south, and southwest regions. Regressions are significant at the 0.01 level.

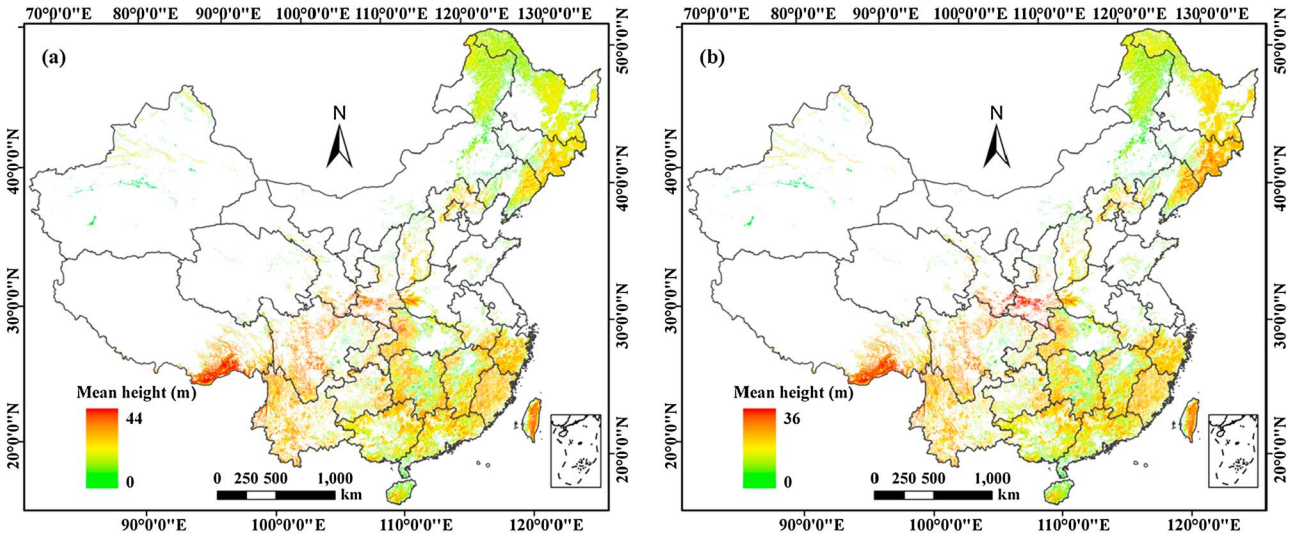

Figure 3. Comparison of forest canopy height in China (a) before and (b) after the calibration.

measurements very well (Figure 2). The respective RMSE and R^2 values are 3.15 m and 0.41 for the northeast and northwest regions and 4.18 m and 0.63 for other regions ($P < 0.01$). The regression slope between remotely sensed and observed height values is here regarded as a correction coefficient. The remotely sensed forest canopy height was converted to the mean forest height by division of 1.2281 and 1.4731 for corresponding regions. In general, forest height is high in the south tropical and subtropical zones, and northeast Changbai Mountains, but low in the north and northwest regions (Figure 3). The calibrated height map (Figure 3b) was used to estimate pixel-based forest stand age in conjunction with a forest type map and an appropriate relationship between stand age and forest height (Table 4).

2.1.4. Forest Inventory Data

Forest inventory data collected as close to the year 2005 as possible, including national, provincial, and county FID, were obtained from the State Forestry Administration. The data were used to validate estimated forest stand age. At the provincial level, the seventh FID for 2004–2008 was employed [*Chinese Ministry of Forestry*, 2009]. This data set provided provincial statistical information on areas and ages of five age classes for dominant forest species. At the plot and stand compartment levels, only some provincial and county inventory data were available, including Heilongjiang (2006), Panshi and Shulan Counties in Jilin (2005), Guangdong (2007), Jiangxi (2006), and Xiamen City in Fujian (2003). These inventories roughly represented forests in the northeast, south, and east regions. The provincial inventory design consists of 0.067 ha plots systematically placed across the forest stands, encompassing a representative range of stand ages, geographic coordinates, mean forest heights, and forest types. The county inventory investigates forest area, forest type, stand age, and mean tree height by stand compartment.

2.2. Methods

2.2.1. Estimating Forest Stand Age

1. Step 1. Fitting the biomass-height relationship
   Tree height, DBH, and volume are the best independent variables for establishing a biomass estimation model. According to the theory of forest growth, forest height is related to DBH and volume, which provide a good theoretical basis for estimating large-scale forest biomass patterns based on the relationship between biomass and forest height. Statistical analysis has been a common method of fitting the biomass-height relationship. Widely used regression models include power [*Chave et al.*, 2005; *Köhler and Huth*, 2010; *Mitchard et al.*, 2011; *Saatchi et al.*, 2011; *Wang et al.*, 2013], linear [*Fang et al.*, 2006; *Skowronski et al.*, 2007], the quadratic polynomial [*Lefsky et al.*, 2005b], and exponential functions [*Yu et al.*, 2010]. Previous studies have shown that biomass-height relationships differ greatly across environmental gradients and among different forest types [*Drake et al.*, 2003; *Pan et al.*, 2004; *Wang et al.*, 2013]. In this study, 2157 sampling plots with both stand biomass (aboveground and belowground) and mean height measurements were first selected from all 3543 sampling plots (Appendix S1 in the supporting information).

Then, different models were fitted to quantify biomass-height relationships for major forest types in different regions of China (Appendix S2 in the supporting information). The optimal models for different forest types in each region were chosen according to the *F* significance test.

2. Step 2. Fitting the stand age-biomass relationship
   According to earlier studies [*Huang*, 2009], five theoretical stand growth models, including Richards, Mitscherlich, Logistic, Gompertz, and Korf models, were selected to describe the relationships between stand biomass and age (Table 1). In this study, forest stand age was calculated by reversing stand growth models, which describe the change of biomass with age. The parameters for stand growth models were estimated by nonlinear regression, using the Levenberg-Marquardt optimization algorithm to minimize the square of absolute differences between forest age observations and estimates. Both stand age and biomass measurements from 3171 field plots were used to fit five types of growth models for different forest types widely distributed in each region of China. The optimal model for each forest type in a region was determined following statistical significance.
3. Step 3. Estimating forest stand age
   To map forest canopy height globally, the Terra MOD44B percent tree cover product from Moderate Resolution Imaging Spectroradiometer (MODIS) was used as a benchmark map [*Simard et al.*, 2011]. In this study, a forest type map produced using Thematic Mapper (TM) data with higher classification accuracy was used. Consequently, there are about 28% of forest pixels in the forest type map with remotely sensed height equal to zero because forest types in these two maps were not completely consistent. They were evenly distributed across China. These zero values were replaced with eight neighboring pixel averages of each center pixel by adopting a "moving window" approach, leaving less than 5% of forest pixels in the forest type map of China with zero values of forest height. However, these pixels were not further processed. Their ages were labeled as no data. According to the biomass-height and age-biomass relationships determined in steps 1 and 2 and the ranges of biomass for the application of function f_1 in Table 1, corresponding relationships between forest age and height in equation (1), and their applicable conditions, were now established. With these relationships and remotely sensed forest height map, the pixel-based forest age was quantitatively estimated. For pixels with forest height beyond the application conditions of age-height relationships, their stand ages were assigned as the corresponding minimal or maximal ages derived from the age-height relationships.

2.2.2. Validating Forest Stand Age

Given the spatial scale of the analysis, it is difficult to conduct a direct validation across the whole of China. Estimates of FID-based stand age directly reflect the dynamics of forest age caused by both disturbed and nondisturbed factors, which can serve as ground truth. Based on national forest inventory data, the mean stand age of each province is calculated as [*Zhao*, 2004]

$$A_i = \frac{1}{S_i}\sum_{m=1}^{n}\sum_{j=1}^{5} S_{mj}A_{mj} \tag{2}$$

where A_i and S_i are the mean stand age and total forest area of province *i*, respectively; S_{mj} and A_{mj} are the area and median age of age class *j* for forest type *m*; and *n* is the number of forest types in province *i*. Then, averages of pixel-based forest ages estimated from remotely sensed forest height were compared with the FID estimates for 31 provinces in China with inventory data available.

For the provincial FID, the plots were regularly distributed on 4 km × 4 km, 8 km × 4 km, and 8 km × 8 km grids, grid size changing among provinces. Therefore, the number of plots falling within a 1 km^2 pixel was one at most. For the county FID, only the whole compartment within a 1 km^2 pixel was used here. When a pixel included more than one stand compartment, an area-weighted mean age was calculated for each 1 km × 1 km pixel. Observed ages from plots and stand compartments were used to validate the estimated ages by way of linear regression.

2.2.3. Uncertainty Analysis of Estimated Forest Stand Age

The uncertainties of currently estimated forest ages were mainly caused by uncertainties in remotely sensed forest canopy height and parameters in the age-height relationships. These parameters were optimized using field measurements. The uncertainties of estimated forest ages related to them would be small. They might be primarily caused by uncertainties in remotely sensed forest height. The validation of corrected remotely sensed forest height using measurements from 263 sampling plots in China yielded a RMSE value of 4.24 m. Therefore, the uncertainties of estimated forest age related to forest height were assessed through deriving equation (1) with the corrected forest height map disturbed by ±1 to 9 m (at an interval of 1 m).

Table 2. Allometric Relationships Between Forest Biomass and Height of Major Forest Types in Different Regions of China[a]

Forest Type	Region	Function f_2	R^2	F	n
DNF	NE	$B = 1.8343H^{1.551}$	0.87	693.65	104
	N, NW	$B = 1.2814H^{1.7539}$	0.80	966.11	242
	E, S, SW	$B = 3.1252H^{1.3588}$	0.79	113.68	33
ENF	NE	$B = 4.041H^{1.4184}$	0.87	1400.00	204
	N	$B = 10.177H$-2.4135	0.69	454.34	208
	E	$B = 3.5069H^{1.4454}$	0.76	849.48	275
	S	$B = 4.5293H^{1.2521}$	0.77	277.82	83
	SW	$B = 2.4046H^{1.6297}$	0.80	256.86	64
	NW	$B = 11.378H + 0.3809$	0.71	270.36	114
DBF	NE	$B = 21.238 \exp(0.0935H)$	0.68	156.17	76
	N	$B = 1.5166H^{1.7134}$	0.61	413.73	278
	NW	$B = 0.9844H^{1.7414}$	0.82	336.54	75
	E, S, SW	$B = 0.759H^{1.6733}$	0.80	205.86	53
EBF	E, N, NE, NW	$B = 3.374H^{1.4748}$	0.63	110.22	67
	S, SW	$B = 1.0782H^{1.7549}$	0.63	179.98	108
MF	N, NE, NW	$B = 3.7994H^{1.3619}$	0.83	206.84	44
	E, S, SW	$B = 5.0308H^{1.3569}$	0.79	490.89	129

[a] f_2 defined in equation (1) represents forest biomass (B, Mg ha^{-1}) as function of forest height (H, m): $B = f_2(H)$. The biomass-height relationships were fitted using field measurements at 2157 plots. All statistics are significant at the 0.01 level. DNF is deciduous needleleaf forest; ENF is evergreen needleleaf forest; DBF is deciduous broadleaf forest; EBF is evergreen broadleaf forest; MF is mixed forest. E, N, NE, NW, S, and SW respectively denote Eastern China, Northern China, Northeastern China, Northwestern China, Southern China and Southwestern China.

In total, 19 forest age maps were generated. Then, the standard deviation for each 1 km pixel was calculated from these 19 age maps and used to characterize the uncertainties in the derived forest age map.

3. Results

3.1. Models for Forest Stand Age Estimation

The optimal biomass-height relationships are shown in Table 2. For all forest types, with the exception of ENF in the north and northwest regions and DBF in the northeast region, the power function performed best in describing biomass-height relationships. The fitted models for all forest types show statistically significant at the 0.01 level with each R^2 greater than 0.60, indicating the applicability of these models to estimating forest biomass according to height in China. Table 3 lists the optimal models for all forest types in each region of China, which predict stand age based on the stand age-biomass relationships. The R^2 values of these models are all above 0.71 ($P < 0.01$), confirming the feasibility of stand growth models for estimating forest age in China.

The high R^2 values of the biomass-height and age-biomass relationships for different forest types in six regions nationwide suggest that the approach taken here may yield viable estimations for China's forest age based on the age-height relationships (Table 4). These relationships depend on the models given in Tables 1–3. For most forest pixels, forest ages can be directly estimated from the remotely sensed forest height map. However, about 17.8% of forest pixels in the forest height map are beyond the scope of the application conditions of age-height relationships, of which the northeast, north, east, south, southwest, and northwest regions respectively account for 3.1%, 4.6%, 3.1%, 0.7%, 4.4%, and 1.9% of the national total forest pixels. The ages of such pixels were assigned the values estimated with the lower or upper boundary height.

3.2. Validation of Estimated Forest Stand Age

3.2.1. Provincial- and Regional-Level Performance

In general, the estimates are in good agreement with the FID values at the provincial and regional levels (Figure 4). However, the biases for Chongqing and Guizhou are respectively 42 and 38 years higher than the FID estimates (Figure 4a). From the point of view of the entire country, these errors are acceptable because forested areas in these two provinces only account for 3.7% of the national total. Forests in Anhui, Fujian, Guangdong, Gansu, Guangxi, Heilongjiang, Hunan, Inner Mongolia, Jiangsu, Jiangxi, Sichuan, Shandong, Shanxi, and Tibet make up 64.5% of the national total forest area, and the biases of provincial mean forest

Table 3. The Fitted Parameters of Forest Age-Biomass Relationships for Different Forest Types in Six Regions of China Based on Stand Growth Models[a]

Forest Type	Region	Model	Parameters			R^2	N	RMSE
			a	b	c			
DNF	NE	G	228.1324	1.3351	0.0755	0.80	157	9.05
	N	G	132.2652	1.6575	0.1047	0.74	231	17.01
	E	L	301.2842	7.3000	0.4351	0.71	24	4.22
	S, SW, NW	L	216.3401	1.8860	0.0429	0.76	26	40.03
ENF	NE	L	187.5991	4.6440	0.1748	0.76	259	18.66
	N	L	83.3676	3.8361	0.2385	0.76	182	9.06
	E	L	217.2470	2.4354	0.1380	0.74	375	6.65
	S	L	305.3722	2.2605	0.0803	0.73	297	8.67
	SW	G	286.5693	0.5818	0.0184	0.74	311	37.21
	NW	G	421.6592	0.9413	0.0156	0.77	184	19.22
DBF	N, NE	G	131.0536	0.7368	0.0235	0.74	225	12.20
	E, S, SW	K	228.2524	10.4064	1.1124	0.81	124	15.37
	NW	L	137.2639	2.8626	0.0834	0.72	61	11.46
EBF	E, N, NE, NW	G	501.6774	0.8718	0.0303	0.75	115	17.71
	S	M	640.7587	0.9270	0.0082	0.79	203	20.00
	SW	G	330.5979	0.7789	0.0270	0.75	188	18.73
MF	N, NE, NW	L	247.0067	5.1220	0.2045	0.82	75	37.25
	E, S, SW	K	451.5684	6.8928	0.6293	0.88	120	6.03

[a]Forest types, regions, and models are identified in Tables 1 and 2. a, b, and c are model parameters given in Table 1. The age-biomass relationships were fitted using field measurements at 3171 plots. RMSE is the root-mean-square error (year). All statistics are significant at the 0.01 level.

ages in these provinces are all no more than 5 years. Henan, Jilin, Shanghai, Shannxi, Yunnan, and Zhejiang have biases of estimated provincial mean forest ages within 6–9 years. Forest areas in these six provinces occupy 22.2% of the national total. In the above 20 provinces, forests account for 86.7% of the national total and the differences between estimated provincial mean forest ages and inventory data are smaller than 10 years. The biases of estimated provincial forest age in Beijing, Hebei, Hubei, Liaoning, and Ningxia are between 11 and 13 years, which cover 7.7% of the national total forest area. In the remaining four provinces with forest area accounting for 1.9% of national total, the departures of estimated provincial mean forest ages from inventory data

Table 4. Relationships Between Forest Age and Height for Different Forest Types in Six Regions of China[a]

Forest Type	Region	Forest Age Formula	Application Conditions
DNF	NE	$A = 17.6834 - 13.245\ln(4.8233 - 1.551\ln(H))$	$1.9339 < H < 22.4166$
	N	$A = 15.8309 - 9.5511\ln(4.6368 - 1.7539\ln(H))$	$0.7065 < H < 14.0653$
	E	$A = 16.7777 - 2.2983\ln(96.4048H^{-1.3588} - 1)$	$0.1339 < H < 28.8526$
	S, SW	$A = 43.9627 - 23.31\ln(69.2244H^{-1.3588} - 1)$	$5.0862 < H < 22.6114$
	NW	$A = 43.9627 - 23.31\ln(168.831H^{-1.7539} - 1)$	$5.8617 < H < 18.6209$
ENF	NE	$A = 26.5675 - 5.7208\ln(46.4239H^{-1.4184} - 1)$	$0.5626 < H < 14.9653$
	N	$A = 16.0843 - 4.1929\ln(83.3676/(10.177H - 2.4135) - 1)$	$0.4102 < H < 8.4289$
	E	$A = 17.6478 - 7.2464\ln(61.9484H^{-1.4454} - 1)$	$3.0398 < H < 17.3706$
	S	$A = 28.1507 - 12.4533\ln(67.4215H^{-1.2521} - 1)$	$4.3864 < H < 28.8792$
	SW	$A = 31.6196 - 54.3478\ln(4.7806 - 1.6297\ln(H))$	$6.2684 < H < 18.7919$
	NW	$A = 60.3397 - 64.1026\ln(6.0442 - \ln(11.378H + 0.3809))$	$2.8219 < H < 37.0258$
DBF	NE	$A = 31.3532 - 42.5532\ln(1.8198 - 0.0935H)$	$0 < H < 19.4631$
	N	$A = 31.3532 - 42.5532\ln(4.4591 - 1.7134\ln(H))$	$3.9874 < H < 13.4973$
	E, S, SW	$A = 8.2131/(5.7062 - 1.6733\ln(H))^{0.899}$	$0 < H < 30.2697$
	NW	$A = 34.3237 - 11.9904\ln(139.4392H^{-1.7414} - 1)$	$3.1889 < H < 17.0378$
EBF	E, N, NE, NW	$A = 28.7723 - 33.0033\ln(5.0019 - 1.4748\ln(H))$	$5.8720 < H < 29.7128$
	S	$A = 778.8843 - 121.9512\ln(640.7587 - 1.0782H^{1.7549})$	$8.5703 < H < 38.0815$
	SW	$A = 28.8481 - 37.037\ln(5.7256 - 1.7549\ln(H))$	$7.5453 < H < 26.1183$
MF	N, NE, SW	$A = 25.0465 - 4.89\ln(65.012H^{-1.3619} - 1)$	$0.4966 < H < 21.4399$
	E, S, SW	$A = 21.4927/(4.4971 - 1.3569\ln(H))^{1.5891}$	$0 < H < 27.5016$

[a]Forest types and regions are identified in Table 2. Forest stand age (A, year) is obtained as function of height (H, m) through replacing biomass in the fifth column function f_1 of Table 1 with function f_2 in Table 2. Application conditions of forest age estimation are calculated according to the ranges of biomass application of function f_1 in Table 1.

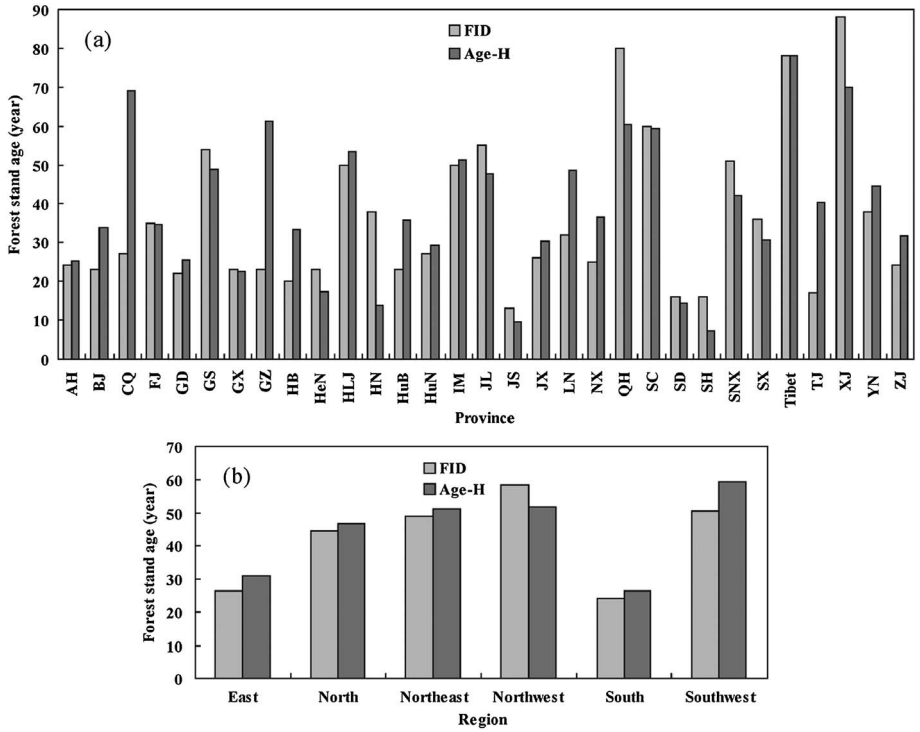

Figure 4. The province-by-province and region-by-region comparisons of estimated forest age based on the relationship between forest age and height (Age-H) with the forest inventory (FID) estimates: (a) provincial scale and (b) regional scale. Province letter designations are stated in the Figure 1 caption.

are within 18 and 24 years. The biases of mean estimated forest ages in six regions are respectively 4, 2, 2, 2, and 8 years older in the east, north, northeast, south, and southwest regions and 7 years younger in the northwest region than the FID estimates (Figure 4b). The northern regions have substantially better results than the southern regions of China. Province-by-province correlation analysis between the age-height estimates and the FID results (Figure 5) indicate that the age-height relationship generally captures the magnitude of forest ages in 31 provinces, with R^2 and RMSE of 0.53 and 12 years (Figure 5a). At the regional scale, the age-height relationship estimates have a better agreement with the FID estimates, with R^2 and RMSE of 0.87 and 4 years (Figure 5b).

The area percentages of different classes of estimated age were further compared with the FID estimates (Figure 6). The estimates of forest age structure using the age-height method are well consistent with the FID estimates in Anhui, Fujian, Guangdong, Gansu, Guangxi, Henan, Heilongjiang, Hubei, Hunan, Inner Mongolia, Jiangsu, Jiangxi, Ningxia, Shandong, Yunnan, and Zhejiang. Forest areas in these 16 provinces constitute 67.6% of the national total. In some regions of north and northeastern plains (Beijing, Hebei, Liaoning, and Tianjin), where

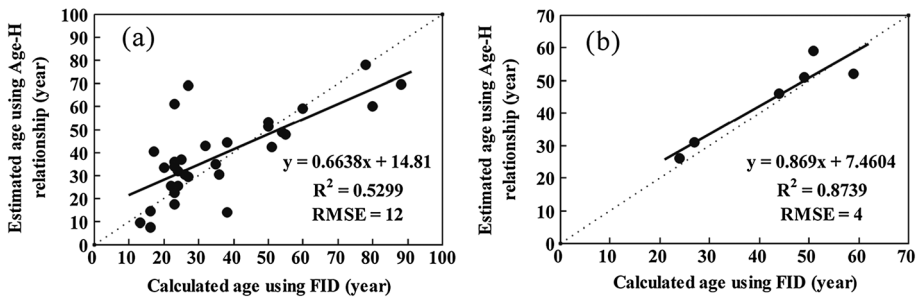

Figure 5. Comparisons of estimated forest age based on relationship between forest age and height (Age-H) and the forest inventory (FID) estimates for 31 provinces and six regions in China: (a) provincial scale and (b) regional scale. The solid line is the regression line, while the dash line is the 1:1 line. RMSE is the root-mean-square error (year). All statistics are significant at the 0.01 level.

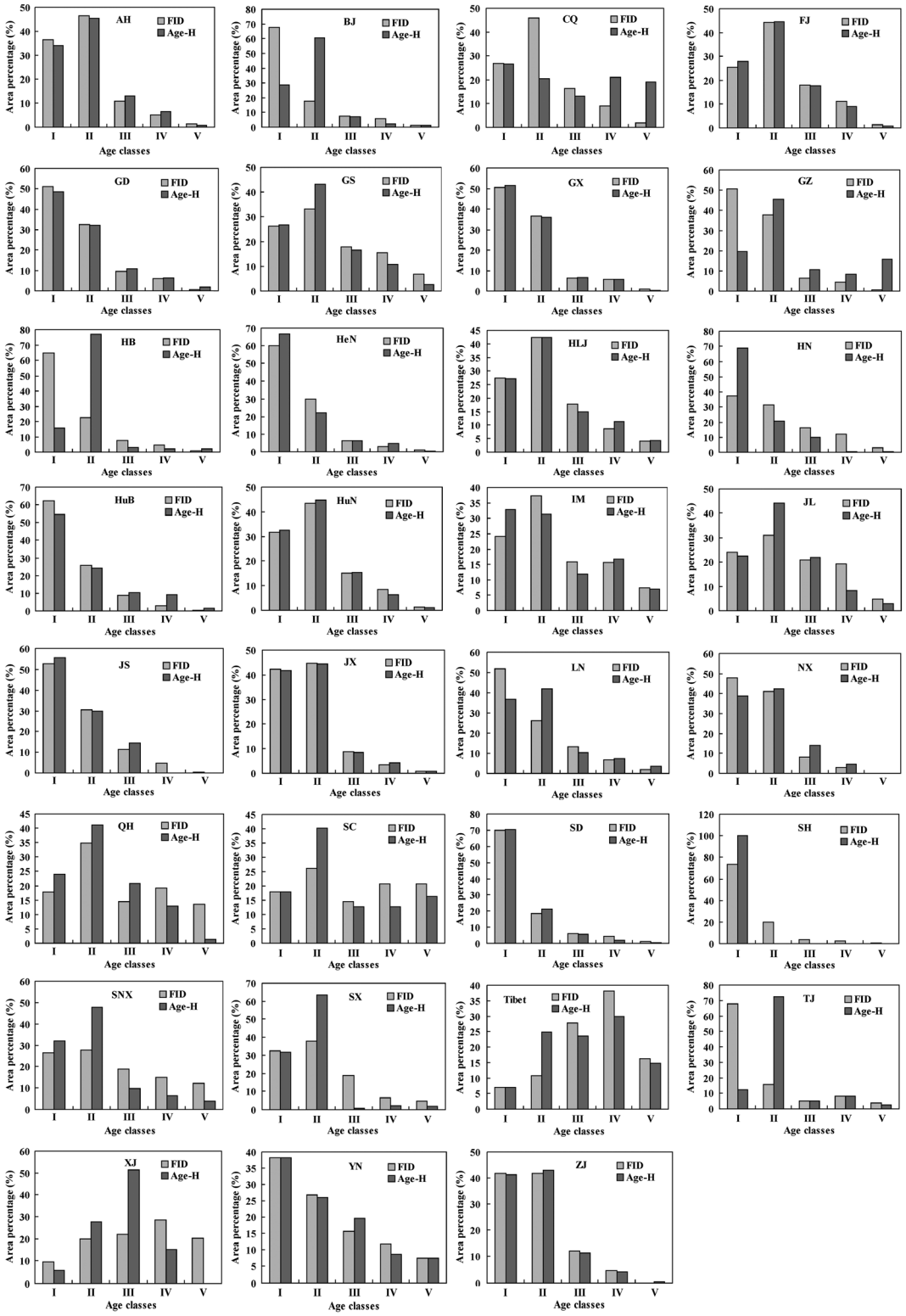

Figure 6. The province-by-province comparisons of estimated forest age for five age classes based on the relationship between forest age and height (Age-H) with forest inventory (FID) estimates. I, II, III, IV, and V denote young, middle-aged, premature, mature, and overmature forests, respectively. Province letter designations are stated in the Figure 1 caption.

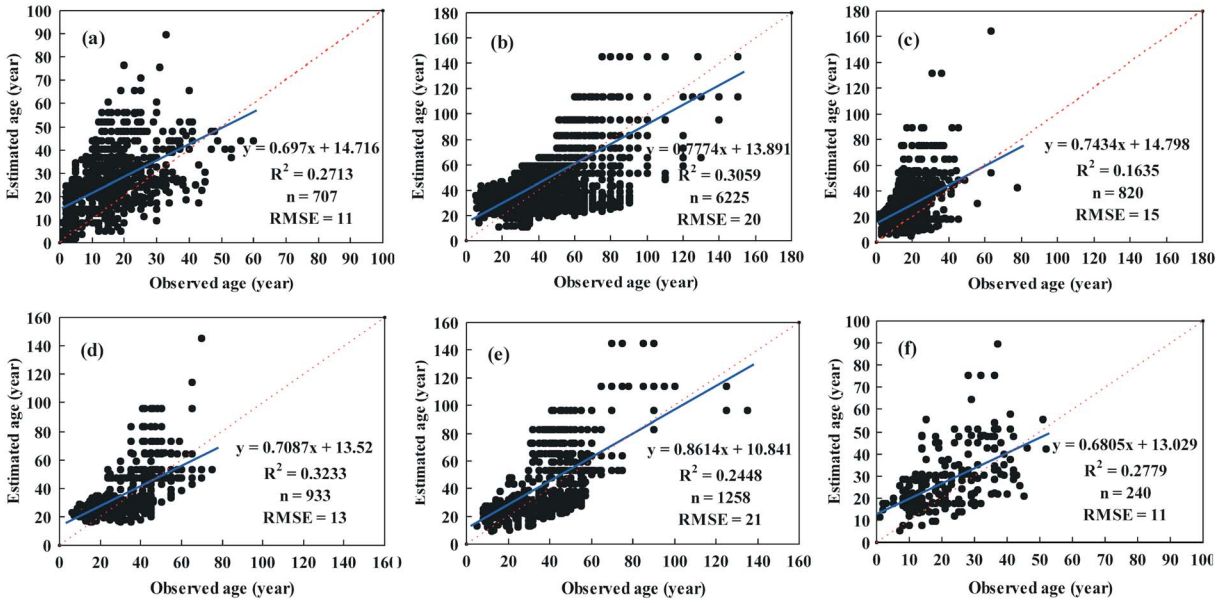

Figure 7. The comparisons of estimated forest age based on the relationship between age and height with observed stand age at the plot scale in some provinces and counties. (a) Guangdong, (b) Heilongjiang, (c) Jiangxi, (d) Panshi, (e) Shulan, and (f) Xiamen. The solid line is the regression line, while the dash line is the 1:1 line. RMSE is the root-mean-square error (year). All statistics are significant at the 0.01 level.

highly populated and most forests are young, the age-height method consistently underestimates the areas of young forests and overestimates the areas of middle-aged forests. For forests spread along the mountain ranges of central China (Sichuan, Shannxi, and Shanxi), there is consistently an overestimate for middle-aged forests and an underestimate for old-aged forests. This is also a similar case to the provinces of Hainan, Jilin, Qinghai, Shanghai, Tibet, and Xinjiang. For forests located in the edge of the Sichuan Basin and the Daba Mountains (Chongqing) and on the outskirt of the Hengduan Mountains system (Guizhou), they bear some similarity with an underestimate for young and middle-aged forests and an overestimate for older forests. The good agreement of estimated forest age with the FID estimates for five age classes at the provincial level further verified the applicability of the method developed here. However, due to some inaccuracy in the forest height map caused by complex topographical and socioeconomic factors, the estimates of forest age in Chongqing, Guizhou, and Tianjin still have large disagreement with the FID estimates.

3.2.2. Pixel Level Performance

Figure 7 presents the comparisons of estimated forest ages with ground observations from the provincial and county FID for three provinces (Figures 7a–7c) and three counties (Figures 7d–7f). The agreement is statistically significant and estimated forest ages are linearly correlated with observations, with a slight overestimate for young forests and an underestimate for old forests. The correlations are moderately high with R^2 values equal to 0.27, 0.31, and 0.16 for the provincial (Guangdong, Heilongjiang, and Jiangxi) inventory and 0.32, 0.24, and 0.28 for the county (Panshi, Shulan, and Xiamen) inventory, respectively. Unfortunately, the estimates were not compared with observations over other parts of the country in such way, especially the southwest and south regions, which contain 46% of the national forest area, because of unavailability of inventory data in these regions. Although there are only three provincial and three county FID sets nationwide for validation, the results encourage general use of the method developed here. It seems that estimated forest age is less accurate at the pixel scale than at regional and provincial scales in view of larger RMSE values ranging from 11 to 21 years. One major reason for this difference is that the ground observations were made at particular sites with sample areas much smaller than 1 km^2 (0.067 ha and 0.267–46.5 ha for provincial and county FID, respectively), while the estimates retrieved from the age-height relationship are the average ages for 1 km^2 areas. At regional and provincial scales, the errors of individual pixels can be cancelled by each other to some extent.

3.3. Spatial Pattern of China's Forest Stand Age

Figure 8 illustrates the distribution of estimated forest ages (Figure 8a) and corresponding uncertainties (Figure 8b). It shows highly spatial heterogeneity of forest age in China, which reflects differences in

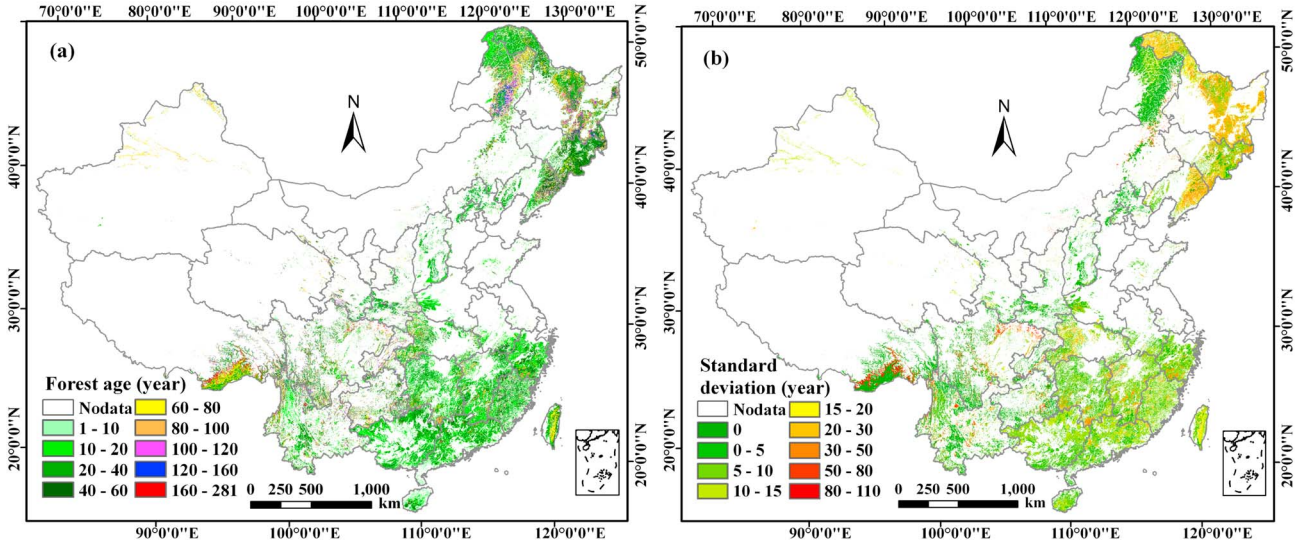

Figure 8. (a) Spatial patterns of China's forest age in 2005 and (b) its standard deviations that examine uncertainty in the age map (the age estimate for Taiwan is based on the same approach for eastern China).

topographical conditions, forest types, and disturbance intensity. Estimated forest age across China ranges from 1 to 281 years, with a mean value of 43 years and standard deviation of 16 years (Figure 8a). Forest age shows definite spatial gradients that increase from the east to the west and from the south to the north. Forests with stand age less than 40 years account for 64% of the national total, primarily located in southern and eastern China owing to intensive previous human disturbances and successful implementation of many national afforestation and reforestation programs since the 1980s [*Fang et al.*, 2001]. Forests between the ages of 40 and 60 years mainly exist in the northeast, southwest, east, and south regions of China, covering 16.3% of the national total. In southeastern Tibet, northeastern Inner Mongolia, northern Heilongjiang and Yunnan, southern Guizhou, and Xinjiang, forests tend to be older because of slow forest growth and relatively low human impact. There the dominant age groups are from 60 to 120 years. Forests with stand age in excess of 120 years mainly appear in the northeast (Daxing'anling, Xiaoxing'anling, and Changbai Mountains) and in the southwest subalpine mountains of China, where natural broadleaf and needleleaf mixed forests are dominantly distributed.

If forests are grouped according to age classes of 1–27, 27–45, 45–65, 65–110, and >110 years, which are classified in the forest inventory as young, middle-aged, premature, mature and overmature forests, respectively, forests within corresponding age class estimated in this study account for 38.2%, 31.2%, 13.1%, 11.3%, and 6.2% of China's total forest area, well consistent with the numbers (33.9%, 33.4%, 14.8%, 12.0%, and 5.9%, respectively) based on the forest inventory [*Chinese Ministry of Forestry*, 2009]. The majority of forests in China are currently young and middle aged, implying large future carbon sequestration potential by forests in China through forest growth and regrowth [*Fang et al.*, 2001; *Pan et al.*, 2004; *Zhang et al.*, 2013].

Figure 8b shows the spatial distribution of estimated uncertainties in retrieved forest age. High uncertainties occur in Hengduan Mountains ranges located in the northeastern part of Tibet Plateau due to high sensitivity of estimated forest age to uncertainties in forest height, complex topographical features, and specific altitudinal gradient for forests ranging from boreal to subtropical. The uncertainties are also high in northeastern China, where newly planted young forests and old forests are widely distributed. In the east, south, and north regions, the uncertainties are mostly about 10 years.

4. Discussion

4.1. Methodology for Forest Stand Age Estimation

Regression analysis has been a widely used method of linking biophysical variables and remote sensing data to obtain continuous estimates of variables such as biomass at global and regional scales [*Cohen et al.*, 2003; *Dong et al.*, 2003; *Saatchi et al.*, 2011]. However, this method has seldom been utilized to map forest age

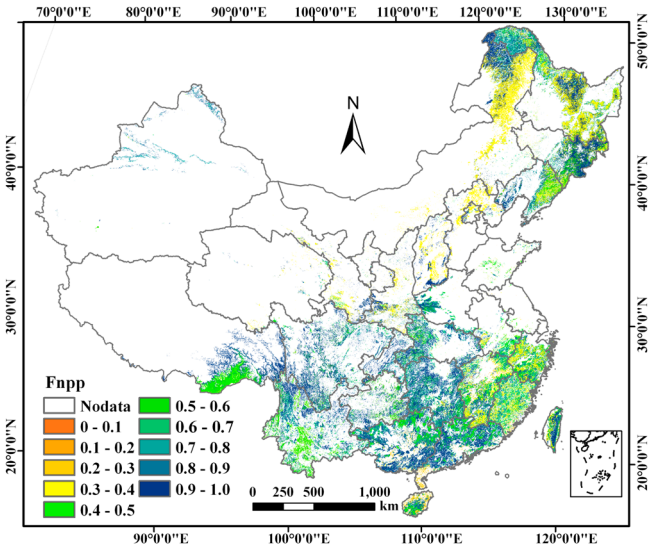

Figure 9. The age effect of forest NPP (Fnpp) derived from the forest age map (Figure 8a) and the NPP-age relationship.

[*Zhang et al.*, 2004; *Dai et al.*, 2011]. Here, forest height was selected as a predictor of forest age. Early studies showed that the relationship between forest age and height could be described using a linear [*Hamilton and Christie*, 1971], exponential [*Fang et al.*, 2006] or logarithmic function [*Bradford et al.*, 2008], which is hard to establish using a uniform expression at present. Forest biomass is highly correlated with both forest age and height. Consequently, it was selected here as an intermediate variable to acquire the relationship between forest age and height. The biomass-height and age-biomass relationships change with regions and forest types, which is taken into account here. The validation indicates that the approach proposed in this study is capable of estimating forest age with acceptable accuracy.

Our estimated forest age was comparable to the national mean value estimated based on FID by *Wang et al.* [2007] and the combined information from FID and remote sensing by *Dai et al.* [2011], respectively. However, the map produced in this study reflects more detailed spatial variations of forest age because of the use of 1 km remotely sensed forest height data and age-height relationships optimized for different forest types in different regions. Forest age, implicitly reflecting the past disturbance legacy, is a simple and direct surrogate for the time since disturbance [*Pan et al.*, 2011a]. The age map produced from detailed inventory data and different sources of data containing information on historical forest disturbance might have high accuracy [*Pan et al.*, 2011a]. However, this method may be not applicable in other areas since spatially distributed inventory and disturbance data are not always available. With the consideration of data availability and urgent requirement for a reliable forest age map in China, remotely sensed forest height is first used to map the forest age distribution in combination with the age-height relationship derived from field observations. This method can, to some extent, alleviate the underestimation of old forest age compared with methods using optical remote sensing data since the LiDAR signal for height detection is less saturated for old forests. In addition, it can be implemented with limited observations of forest biomass, height, and age. Therefore, this method can be widely utilized for many regional applications. In this case, the age estimates are for the year 2005. In future, the approach might be used to estimate regional-scale and national-scale forest age on a yearly basis if annual remotely sensed forest height data are available.

4.2. Implications of the Forest Stand Age Map

Age-related changes in forest productivity have been recognized for many years. Recent flux measurements further confirmed the age effect on NEP [*Coursolle et al.*, 2012]. However, NEP cannot be directly estimated from the age information. *Chen et al.* [2003] developed a general semiempirical function to describe the change of NPP with age [*Chen et al.*, 2003; *Wang et al.*, 2011; *Zhang et al.*, 2012]. The effects of stand age on NPP and NEP could be quantified using forest age and the generalized NPP-age relationship (Fnpp) [*Pan et al.*, 2011a; *Deng et al.*, 2013]. Figure 9 shows the Fnpp values of forests in China derived from the forest age map (Figure 8a) and NPP-age relationships fitted using field measurements (Appendix S3 in the supporting information). Low values (<0.4) indicate low productivity because of young or old forest ages, which are acting as carbon sources (NEP < 0). Forests with high productivity (Fnpp > 0.7) normally act as large carbon sinks (NEP > 0) and are widely distributed in most areas of China. This is consistent with outputs from many previous studies [*Fang et al.*, 2001; *Piao et al.*, 2005; *Wang et al.*, 2007]. With this map, atmospheric inversion of terrestrial carbon flux can be improved [*Deng et al.*, 2013]. It can also be used to optimize management strategy for enhancing carbon sequestration and maximizing the profit of forestry [*Pan et al.*, 2011a].

Forest age structure greatly affects the magnitude and spatial distribution of regional carbon budget. It has been incorporated into distinct modeling approaches, i.e., forest inventory [*Kurz and Apps*, 1999; *Pan et al.*, 2011a], process-based models [*Chen et al.*, 2000], and atmospheric CO_2 inversions [*Deng et al.*, 2013], for improving carbon budget estimation [*Ju et al.*, 2007; *Zhang et al.*, 2012]. Many studies [*Fang et al.*, 2001; *Piao et al.*, 2005; *Wang et al.*, 2007; *Pan et al.*, 2011b] indicated that forests in China have been acting as a carbon sink in recent decades. However, the magnitudes of this sink varied considerably in different studies. Carbon budget estimation is very sensitive to forest age. The errors of 5 years in forest age might cause uncertainties of 12–22% and 5–9% in simulated net biome productivity and NPP, respectively [*Chen et al.*, 2003]. The resulting age map with high quality will be beneficial for improving the estimation of carbon budget and the projection of its future trend for China's forests.

4.3. Uncertainty and Major Error Sources of Forest Stand Age

Forest ages estimated using the age-height relationships require adequate and representative field measurements. If the relationship could not be established for a certain forest type in a region due to the unavailability of field data, relationships from a neighboring region were adopted. In addition, field-measured forest height values of sampling plots for several forest types varied in a much smaller range than the remotely sensed values, notably for DBF in the northeast (3.60–17.50 m versus 4.88–27.69 m) and north regions (4.00–16.00 m versus 2.71−25.80 m) (Appendices S1 and S2 in the supporting information). Thus, height values of some pixels in the forest height map were beyond the boundary conditions that the age-height relations are applicable. The ages for these pixels were assigned the values estimated with the lower or upper boundary height. Due to such simplification, the stand age for old forests might be underestimated in areas of Jilin and Shanxi (Figure 4). Fortunately, only 5.9% of forests are presently overmature in China [*Chinese Ministry of Forestry*, 2009]. Consequently, the spatial pattern of forest age would have not been significantly affected, despite the possibility of slight underestimation of forest age for old forests.

The forest height map employed here is one of the best descriptions of forest vertical structure at regional and global scales currently available [*Simard et al.*, 2011]. Its estimates are highly variable due to the impacts of forest heterogeneity and topography [*Lefsky et al.*, 2005b; *Duncanson et al.*, 2010; *Simard et al.*, 2011]. The uncertainties of forest age calculated using this forest height map plus perturbations of ±1 –9 m range from less than 15 years in most regions to more than 50 years in southeastern Tibet and northeastern Sichuan (Figure 8b), indicating high sensitivity of estimated forest age to forest height. Therefore, calibration of the remotely sensed forest height against more ground data is needed. In this study, only two coefficients across the whole of China are fitted to correct the remotely sensed forest canopy height product for different regions. In reality, the errors of remotely sensed forest height might change spatially. Determining the correction coefficient for each region or province could further remedy the bias in the remotely sensed forest height and consequently improve the estimation of forest age. Large errors in age estimation for Chongqing and Guizhou primarily resulted from an overestimate of forest height induced by rough terrains and heterogeneous forests [*Tian et al.*, 2011]. Forest height is also influenced by increasing human disturbance and urbanization (such as Beijing, Hebei, Liaoning, and Tianjin). They all make the estimates of forest age difficult because of the complicated forest structure. Forest height is the predictor of forest age. So more efforts are required to improve the forest height map and thus reduce uncertainties of forest age estimation.

Validation of pixel-based forest age is a real challenge. In this study, different types of FID were used as benchmarks to validate the resulting age map. The national FID does not include age observations per se, so forest age in each province or region was estimated as the area-weighted mean of the median value of different age classes for all forest types. This is a widely used method for calculating mean forest age from national statistical inventory data. However, the mean forest age calculated in this way might include some uncertainties if the forest ages are not evenly distributed in each age class. At present, there is essentially no effective approach to validate model results using plot measurements because of the mismatch of scales between field observations and model estimate. The performance of the model estimates at the individual pixel level is likely to vary with the number of available field observations [*Jenkins et al.*, 2001; *Zheng et al.*, 2003]. Only observations of one plot from the provincial FID and one to several compartments from the county FID were used to validate the average ages of 1 km pixels. These might influence the validation

performance of the resulting age map at the plot and compartments levels. However, it should be kept in mind that the provincial and county FID bases are currently the best data sets available to validate estimated pixel-based forest age because they provide explicit information on the spatial distribution of forest age. In this study, the validation of estimated forest age using spatially distributed provincial and county FID bases is far from sufficient, especially in the southwest and south regions, with approximately 50% of the national total forest area.

The quantitative assessment of uncertainties for the estimated forest age is a challenge and important for proper applications of this map. The uncertainties were quantified using the standard deviations of estimated forest ages, which were generated through perturbing remotely sensed forest height. This implicitly assumes that the fitted age-height relationships are perfect and the errors of remotely sensed forest height are spatially invariant. Such assumptions are not always valid. The uncertainties estimated in this way are only the first order of approximation.

The forest age map derived here is only a metadata-based result. In many cases, trees have different ages in a pixel of 1 km resolution, so the forest age assigned by a single value may not be practical unless there is a very distinct disturbance and regeneration activity, such as a clear-cut followed by newly planted forests [*Bradford et al.*, 2008; *Pan et al.*, 2011a]. The resulting map is most appropriate for large-scale studies and forests with a relatively even-aged stand structure. Forests undisturbed for long periods of time tend to develop an uneven-aged stand structure as canopy gaps become filled with younger trees [*Pregitzer and Euskirchen*, 2004; *Luyssaert et al.*, 2008]. In such mosaic forest structures, LiDAR points are more likely to miss tall trees, resulting in an underestimate of the forest height for old forests [*Simard et al.*, 2011]. On the other hand, probably due to the presence of snags and stumps in the small stands, LiDAR-derived height for young forests might be overestimated [*Lefsky et al.*, 2005a]. It is important to account for age overestimation in young forests and underestimation in old forests. The method used here to estimate stand age from mean tree age would have different effects on age estimation at each stage of forest growth [*Bradford et al.*, 2008].

5. Conclusions

In this paper, the forest age map in 2005 was produced using a calibrated forest height map and the age-height relationships indirectly obtained from field observations for major forest types in different regions of China. The following conclusions can be drawn:

1. Our estimated results match the FID estimates very well, with a R^2 of 0.87, a RMSE of 4 years, and 2–8 years biases for mean forest ages in different regions and a R^2 of 0.53 and a RMSE of 12 years for provincial mean forest ages. In provinces with 86.7% of national total forests, the difference between retrieved and FID-based provincial mean ages are less than 10 years. The validation using provincial and county FID also show the significant agreement between retrieved forest age and ground truth. These results indicate that remotely sensed forest height combined with age-height relationships can act as a practically useful tool to map forest age over large areas.
2. The spatial pattern of forest age in China showed significant heterogeneity. In southern and eastern China, most forest stand age was less than 40 years. Forests more than 120 years old were mainly in the northeast mountains and the southwest subalpine mountains of China, accounting for 4.7% of the total forest area. In southeastern Tibet, Xinjiang, northern Heilongjiang and Yunnan, northeastern Inner Mongolia, and southern Guizhou, forest ages were mostly between 60 and 120 years. The forest age and its standard deviation averaged 43 and 16 years in China.

This study is the first attempt to map forest age distribution based on forest height and observation data. It shows promising results and provides a benchmark map for characterizing forest carbon dynamics accurately, evaluating disturbance impacts, and predicting future forest carbon sequestration potential. However, the estimates of forest age using empirical methods are usually coupled with high uncertainties, largely arising from great spatial variability in age distribution, inadequate field plots, the forest height map of limited quality, and the restricted applicability of the age-height relationship at different scales. Reducing such sources of uncertainty depends on improving the quality of data used to estimate forest age.

Acknowledgments

This study is supported by the National Basic Research Program of China (973 Program) (2010CB950702 and 2010CB833503), the program B for Outstanding PhD candidate of Nanjing University (201301B010), Jiangsu Graduate Innovation Program (CXZZ11_0033), and the Priority Academic Program Development of Jiangsu Higher Education Institutions. We gratefully acknowledge the constructive suggestions by two anonymous reviewers, which greatly helped to improve the quality of this paper.

References

Amiro, B. D., and J. M. Chen (2003), Dating forest fire scars using SPOTVEGETATION for Canadian ecoregions, *Can. J. For. Res.*, *33*, 1116–1125.

Bonan, G. B. (2008), Forests and climate change: Forcings, feedbacks, and the climate benefits of forests, *Science*, *320*, 1444–1449, doi:10.1126/science.1155121.

Bradford, J. B., R. A. Birdsey, L. A. Joyce, and M. G. Ryan (2008), Tree age, disturbance history, and carbon stocks and fluxes in subalpine Rocky Mountain forests, *Global Change Biol.*, *14*, 2882–2897, doi:10.1111/j.1365-2486.2008.01686.x.

Charles, P. W. (1932), The Gompertz curve as a growth curve, *Proc. Natl. Acad. Sci. U.S.A.*, *18*(1), 1–8.

Chave, J., et al. (2005), Tree allometry and improved estimation of carbon stocks and balance in tropical forests, *Oecologia*, *145*, 87–99, doi:10.1007/s00442-005-0100-x.

Chen, J. M., W. J. Chen, J. Liu, J. Cihlar, and S. Gray (2000), Annual carbon balance of Canada's forests during 1895–1996, *Global Biogeochem. Cycles*, *14*, 839–849, doi:10.1029/1999GB001207.

Chen, J. M., W. M. Ju, J. Cihlar, D. Price, J. Liu, W. J. Chen, J. J. Pan, A. Black, and A. Barr (2003), Spatial distribution of carbon sources and sinks in Canada's Forests, *Tellus, Ser. B*, *55*, 622–641, doi:10.1034/j.1600-0889.2003.00036.x.

Chen, W. J., J. M. Chen, D. T. Price, and J. Cihlar (2002), Effects of stand age on net primary productivity of boreal black spruce forests in Ontario, Canada, *Can. J. For. Res.*, *32*, 833–842.

Chinese Ministry of Forestry (2009), *Forest Resource Statistics of China (2004–2008)*, Department of Forest Resource and Management, Chinese Ministry of Forestry, Beijing, China.

Cienciala, E., J. Apltauer, E. Exnerová, and F. Tatarinov (2008), Biomass functions applicable to oak trees grown in Central-European forestry, *J. For. Sci.*, *54*, 109–120.

Cohen, W. B., T. K. Maiersperger, S. T. Gower, and D. P. Turner (2003), An improved strategy for regression of biophysical variables and Landsat ETM+ data, *Remote Sens. Environ.*, *84*, 561–571.

Coursolle, C., et al. (2012), Influence of stand age on the magnitude and seasonality of carbon fluxes in Canadian forests, *Agric. For. Meteorol.*, *165*, 136–148.

Dai, M., T. Zhou, L. L. Yang, and G. S. Jia (2011), Spatial pattern of forest ages in China retrieved from national-level inventory and remote sensing imageries, *Geogr. Res.*, *30*(1), 172–184.

Deng, F., J. M. Chen, Y. Pan, W. Peters, R. Birdsey, K. McCullough, and J. Xiao (2013), Forest stand age information improves an inverse North American carbon flux estimate, *Biogeosci. Discuss.*, *10*, 4781–4817.

Dong, J., R. K. Kaufmann, R. B. Myneni, C. J. Tucker, P. E. Kauppi, J. Liski, W. Buermann, V. Alexeyev, and M. K. Hughes (2003), Remote sensing estimates of boreal and temperate forest woody biomass: Carbon pools, sources and sink, *Remote Sens. Environ.*, *84*, 393–410.

Drake, J. B., R. G. Knox, R. O. Dubayah, D. B. Clark, R. Condit, J. B. Blair, and M. Hofton (2003), Above-ground biomass estimation in closed canopy Neotropical forests using lidar remote sensing: Factors affecting the generality of relationships, *Global Ecol. Biogeogr.*, *12*, 147–159, doi:10.1046/j.1466-822X.2003.00010.x.

Drake, J. E., S. C. Davis, L. M. Raetz, and E. H. DeLucia (2011), Mechanisms of age-related changes in forest production: The influence of physiological and successional changes, *Global Change Biol.*, *17*, 1522–1535, doi:10.1111/j.1365-2486.2010.02342.x.

Drezet, P. M. L., and S. Quegan (2007), Satellite-based radar mapping of British forest age and net ecosystem exchange using ERS tandem coherence, *For. Ecol. Manage.*, *238*, 65–80, doi:10.1016/j.foreco.2006.09.088.

Duncanson, L. I., K. O. Niemann, and M. A. Wulder (2010), Estimating forest canopy height and terrain relief from GLAS waveform metrics, *Remote Sens. Environ.*, *114*(1), 138–154, doi:10.1016/j.rse.2009.08.018.

Fang, J. Y., A. P. Chen, C. H. Peng, S. Q. Zhao, and L. J. Ci (2001), Changes in forest biomass carbon storage in China between 1949 and 1998, *Science*, *292*, 2320–2322, doi:10.1126/science.1058629.

Fang, J. Y., S. Brown, Y. H. Tang, G.-J. Nabuurs, X. P. Wang, and H. H. Shen (2006), Overestimated biomass carbon pools of the northern mid- and high latitude forests, *Clim. Change*, *74*, 355–368, doi:10.1007/s10584-005-9028-8.

Fraser, R. H., and Z. Li (2002), Estimating fire-related parameters in boreal forest using SPOT VEGETATION, *Remote Sens. Environ.*, *82*, 95–110.

Gadow, K. v., and G. Hui (1998), Modeling forest development, Fac. of For. and Woodl. Ecol., Univ. of Göttingen, Germany.

Grace, J. (2004), Age-related dynamics of carbon exchange in European forests: Final report and technical implementation plan, *Tech. Rep.*, University of Edinburgh.

Hamilton, G. J., and J. M. Christie (1971), *Forest Management Tables*, Forestry Commission Handbook, Number 34, H.M. Stationery Off., London, U. K.

He, L. M., J. M. Chen, S. L. Zhang, G. Gomez, Y. D. Pan, K. McCullough, R. Birdsey, and J. G. Masek (2011), Normalized algorithm for mapping and dating forest disturbances and regrowth for the United States, *Int. J. Appl. Earth Obs.*, *13*, 236–245, doi:10.1016/j.jag.2010.12.003.

He, L. M., J. M. Chen, Y. D. Pan, R. Birdsey, and J. Kattge (2012), Relationships between net primary productivity and forest stand age in U.S. forests, *Global Biogeochem. Cycles*, *26*, GB3009, doi:10.1029/2010GB003942.

Houghton, R. A. (2007), Balancing the global carbon budget, *Annu. Rev. Earth Planet. Sci.*, *35*, 313–347, doi:10.1146/annurev.earth.35.031306.140057.

Houghton, R. A., D. L. Skole, C. A. Nobre, J. L. Hackler, K. T. Lawrence, and W. H. Chomentowski (2000), Annual fluxes of carbon from deforestation and regrowth in the Brazilian Amazon, *Nature*, *403*, 301–304, doi:10.1038/35002062.

Huang, L. (2009), The carbon sequestration of afforestation in red soil hilly region in southern China, PhD dissertation, Inst. of Geogr. Sci. and Nat. Resour. Res., Chin. Acad. Sci., Beijing, China.

Jenkins, J. C., R. A. Birdsey, and Y. D. Pan (2001), Biomass and NPP estimation for the mid-Atlantic region (USA) using plot-level forest inventory data, *Ecol. Appl.*, *11*(4), 1174–1193.

Ju, W. M., J. M. Chen, D. Harvey, and S. Wang (2007), Future carbon balance of China's forests under climate change and increasing CO_2, *J. Environ. Manage.*, *85*(3), 538–562, doi:10.1016/j.jenvman.2006.04.028.

Köhler, P., and A. Huth (2010), Towards ground-truthing of spaceborne estimates of above-ground life biomass and leaf area index in tropical rain forests, *Biogeosciences*, *7*(8), 2531–2543, doi:10.5194/bg-7-2531-2010.

Kurz, W. A., and M. J. Apps (1999), A 70-year retrospective analysis of carbon fluxes in the Canadian forest sector, *Ecol. Modell.*, *9*, 526–547.

Lefsky, M. A. (2010), A global forest canopy height map from the Moderate Resolution Imaging Spectroradiometer and the Geoscience Laser Altimeter System, *Geophys. Res. Lett.*, *37*, L15401, doi:10.1029/2010GL043622.

Lefsky, M. A., D. J. Harding, M. Keller, W. B. Cohen, C. C. Carabajal, F. Del Bom Espirito-Santo, M. O. Hunter, and R. de Oliveira Jr. (2005a), Estimates of forest canopy height and aboveground biomass using ICESat, *Geophys. Res. Lett.*, *32*, L22S02, doi:10.1029/2005GL023971.

Lefsky, M. A., T. D. P. Turner, M. Guzy, and W. B. Cohen (2005b), Combining lidar estimates of aboveground biomes and Landsat estimates of stand age for spatially extensive validation of modeled forest productivity, *Remote Sens. Environ.*, *95*, 549–558, doi:10.1016/j.rse.2004.12.022.

Lefsky, M. A., M. Keller, P. Yong, P. B. De Camargo, and M. O. Hunter (2007), Revised method for forest canopy height estimation from Geoscience Laser Altimeter System waveforms, *J. Appl. Remote Sens.*, *1*, 013537, doi:10.1117/1.2795724.

Li, D. Q., W. M. Ju, W. Y. Fan, and Z. J. Gu (2014), Estimating the age of deciduous forests in northeast China with Enhanced Thematic Mapper Plus data acquired in different phonological seasons, *J. Appl. Remote Sens.*, *8*(1), 083670, doi:10.1117/1.JRS.8.083670.
Lucas, R. M., M. Honzak, G. M. Foody, P. J. Curran, and C. Corves (1993), Characterising tropical secondary forests using multi-temporal Landsat sensor imagery, *Int. J. Remote Sens.*, *14*, 3061–3067, doi:10.1080/01431169308904419.
Lucas, R. M., X. Xiao, S. Hagen, and S. Frokling (2002), Evaluating TERRA-1 MODIS data for discrimination of tropical secondary forest regeneration stages in the Brazilian Legal Amazon, *Geophys. Res. Lett.*, *29*(8), 1200, doi:10.1029/2001GL013375.
Luyssaert, S., E. D. Schulze, A. Börner, A. Knohl, D. Hessenmöller, B. E. Law, P. Ciais, and J. Grace (2008), Old-growth forests as global carbon sinks, *Nature*, *455*, 213–215, doi:10.1038/nature07276.
McMillan, A. M. S., and M. L. Goulden (2008), Age-dependent variation in the biophysical properties of boreal forests, *Global Biogeochem. Cycles*, *22*, GB2019, doi:10.1029/2007GB003038.
Mitchard, E. T. A., et al. (2011), Mapping tropical forest biomass with radar and spaceborne LiDAR: Overcoming problems of high biomass and persistent cloud, *Biogeosci. Discuss.*, *8*(4), 8781–8815, doi:10.5194/bgd-8-8781-2011.
Pan, Y. D., T. X. Luo, R. Birdsey, J. Hom, and J. Melillo (2004), New estimates of carbon storage and sequestration in China's forests: Effects of age-class and method on inventory-based carbon estimation, *Clim. Change*, *67*, 211–236, doi:10.1007/s10584-004-2799-5.
Pan, Y. D., J. M. Chen, R. Birdsey, K. McCullough, L. He, and F. Deng (2011a), Age structure and disturbance legacy of North American forests, *Biogeosciences*, *8*, 715–732, doi:10.5194/bg-8-715-2011.
Pan, Y. D., R. A. Birdsey, J. Y. Fang, R. A. Houghton, P. E. Kauppi, and W. A. Kurz (2011b), A large and persistent carbon sink in the world's forests, *Science*, *333*, 988–993, doi:10.1126/science.1201609.
Piao, S. L., J. Y. Fang, B. Zhu, and K. Tan (2005), Forest biomass carbon stocks in China over the past 2 decades: Estimation based on integrated inventory and satellite data, *J. Geophys. Res.*, *110*, G01006, doi:10.1029/2005JG000014.
Piao, S. L., J. Y. Fang, P. Ciais, P. Peylin, Y. Huang, S. Sitch, and T. Wang (2009), The carbon balance of terrestrial ecosystems in China, *Nature*, *458*, 1009–1013, doi:10.1038/nature07944.
Pienaar, L. V., and K. J. Turnbull (1973), The Chapman-Richards generalization of Von Bertalanffy's growth model for basal area growth and yield in even-aged stands, *For. Sci.*, *19*, 2–22.
Pregitzer, K. S., and E. S. Euskirchen (2004), Carbon cycling and storage in world forests: Biome patterns related to forest age, *Global Change Biol.*, *10*, 2052–2077, doi:10.1111/j.1365-2486.2004.00866.x.
Richer, W. E. (1979), Growth rates and models, *Fish Physiol.*, *8*, 677–743.
Ryan, M. G., D. Binkley, and J. H. Fownes (1997), Age-related decline in forest productivity: Pattern and process, *Adv. Ecol. Res.*, *27*(27), 213–262.
Saatchi, S. S., et al. (2011), Benchmark map of forest carbon stocks in tropical regions across three continents, *Proc. Natl. Acad. Sci. U.S.A.*, *108*(24), 9899–9904, doi:10.1073/pnas.1019576108.
Sader, S. A., R. B. Waide, W. T. Lawrence, and A. T. Joyce (1989), Tropical forest biomass and successional age class relationships to a vegetation index derived from Landsat-TM data, *Remote Sens. Environ.*, *28*, 143–156.
Simard, M., N. Pinto, J. B. Fisher, and A. Baccini (2011), Mapping forest canopy height globally with spaceborne lidar, *J. Geophys. Res.*, *116*, G04021, doi:10.1029/2011JG001708.
Skowronski, N., K. Clark, R. Nelson, J. Hom, and M. Patterson (2007), Remotely sensed measurements of forest structure and fuel loads in the Pinelands of New Jersey, *Remote Sens. Environ.*, *108*(2), 123–129, doi:10.1016/j.rse.2006.09.032.
Song, C. H., and C. E. Woodcock (2003), A regional forest ecosystem carbon budget model: Impacts of forest age structure and land use history, *Ecol. Modell.*, *164*(1), 33–47, doi:10.1016/S0304-3800(03)00013-9.
Tian, X. L., J. Xia, H. B. Xia, and J. Ni (2011), Forest biomass and its spatial pattern in Guizhou Province, *Chin. J. Appl. Ecol.*, *22*(2), 287–294.
Turner, D. P., D. Ritts, B. E. Law, W. Cohen, Z. Yang, T. Hudiburg, J. L. Campbell, and M. Duane (2007), Scaling net ecosystem production and net biome production over a heterogeneous region in the western United States, *Biogeosciences*, *4*, 597–612, doi:10.5194/bgd-4-1093-2007.
Vilén, T., K. Gunia, P. J. Verkerk, R. Seidl, M.-J. Schelhaas, M. Lindner, and V. Bellassen (2012), Reconstructed forest age structure in Europe 1950–2010, *For. Ecol. Manage.*, *286*, 203–218, doi:10.1016/j.foreco.2012.08.048.
Wang, S. Q., J. M. Chen, W. M. Ju, X. Feng, M. Chen, P. Chen, and G. Yu (2007), Carbon sinks and sources in China's forests during 1901–2001, *J. Environ. Manage.*, *85*, 524–537, doi:10.1016/j.jenvman.2006.09.019.
Wang, S. Q., L. Zhou, J. M. Chen, W. M. Ju, X. F. Feng, and W. X. Wu (2011), Relationship between net primary productivity and stand age for several forest types and their influence on China's carbon balance, *J. Environ. Manage.*, *92*, 1651–1662, doi:10.1016/j.jenvman.2011.01.024.
Wang, X. P., S. Ouyang, O. J. Sun, and J. Y. Fang (2013), Forest biomass patterns across northeast China are strongly shaped by forest height, *For. Ecol. Manage.*, *293*, 149–160, doi:10.1016/j.foreco.2013.01.001.
Xu, B., Z. D. Guo, S. L. Piao, and J. Y. Fang (2010), Biomass carbon stocks in China's forests between 2000 and 2050: A prediction based on forest biomass-age relationships, *Sci. China Life Sci.*, *53*(7), 776–783, doi:10.1007/s11427-010-4030-4.
Xu, C. Y., M. H. Turnbull, D. T. Tissue, J. D. Lewis, R. Carson, W. S. F. Schuster, D. Whitehead, A. S. Walcroft, J. B. Li, and K. L. Griffin (2012), Age-related decline of stand biomass accumulation is primarily due to mortality and not to reduction in NPP associated with individual tree physiology, tree growth or stand structure in a *Quercus*-dominated forest, *J. Ecol.*, *100*, 428–440.
Yu, Y. F., S. Saatchi, L. S. Heath, E. LaPoint, R. Myneni, and Y. Knyazikhin (2010), Regional distribution of forest height and biomass from multisensor data fusion, *J. Geophys. Res.*, *115*, G00E12, doi:10.1029/2009JG000995.
Zeide, B. (1989), Accuracy of equations describing diameter growth, *Can. J. For. Res.*, *19*(10), 1283–1286.
Zhang, C. H., W. M. Ju, J. M. Chen, M. Zan, D. Q. Li, Y. L. Zhou, and X. Q. Wang (2013), China's forest biomass carbon sink based on seven inventories from 1973 to 2008, *Clim. Change*, *118*, 933–948, doi:10.1007/s10584-012-0666-3.
Zhang, F. M., J. M. Chen, Y. D. Pan, R. A. Birdsey, S. H. Shen, W. M. Ju, and L. M. He (2012), Attributing carbon changes in conterminous U.S. forests to disturbance and non-disturbance factors from 1901 to 2010, *J. Geophys. Res.*, *117*, G02021, doi:10.1029/2011JG001930.
Zhang, Q. F., G. Pavlic, W. J. Chen, R. Latifovic, R. Fraser, and J. Cihlar (2004), Deriving stand age distribution in boreal forests using SPOT VEGETATION and NOAA AVHRR imagery, *Remote Sens. Environ.*, *91*, 405–418, doi:10.1016/j.rse.2004.04.004.
Zhang, Z. X., X. Wang, C. Y. Wang, L. J. Zuo, Q. K. Wen, T. T. Dong, X. L. Zhao, B. Liu, and L. Yi (2009), National land cover mapping by remote sensing under the control of interpreted data, *J. Geo-information Sci.*, *11*(2), 216–224.
Zhao, M. (2004), Study on carbon storage and balance of Chinese main forest ecosystems, PhD dissertation, Grad. Univ. of Chin. Acad. of Sci., Beijing, China.
Zheng, D. L., S. Prince, and R. Wright (2003), Terrestrial net primary production estimates for 0.5 grid cells from field observations—A contribution to global biogeochemical modeling, *Global Change Biol.*, *9*, 46–64, doi:10.1046/j.1365-2486.2003.00534.x.
Zheng, D. L., J. Rademacher, J. Q. Chen, T. Crow, M. Bresee, J. Le Moine, and S. R. Ryu (2004), Estimating aboveground biomass using Landsat 7 ETM+ data across a managed landscape in northern Wisconsin, USA, *Remote Sens. Environ.*, *93*(3), 402–411, doi:10.1016/j.rse.2004.08.008.